



## A zero-equation turbulence model for indoor airflow simulation

Qingyan Chen \*, Weiran Xu

*Building Technology Program, Department of Architecture, Massachusetts Institute of Technology, Room 5-418, 77 Massachusetts Avenue, Cambridge, MA 02139-4307, USA*

Received 8 January 1996

---

### Abstract

At present, Computational-Fluid-Dynamics (CFD) with the 'standard'  $k-\epsilon$  model is a popular method for numerical simulation of room airflow. The  $k-\epsilon$  model needs a lot of computing time and large a computer. This paper proposes a new zero-equation model to simulate three-dimensional distributions of air velocity, temperature, and contaminant concentrations in rooms. The method assumes turbulent viscosity to be a function of length-scale and local mean velocity. The new model has been used to predict natural convection, forced convection, mixed convection, and displacement ventilation in a room. The results agree reasonably with experimental data and the results obtained by the standard  $k-\epsilon$  model. The zero-equation model uses much less computer memory and the computing speed is at least 10 times faster, compared with the  $k-\epsilon$  model. The grid size can often be reduced so that the computing time needed for a three-dimensional case can be a few minutes on a PC. © 1998 Elsevier Science S.A. All rights reserved.

*Keywords:* Computational-fluid-dynamics; Convection; Concentration

---

### 1. Introduction

Proper design of indoor environment requires detailed information of indoor air distribution, such as airflow pattern, velocity, temperature, and contaminant concentrations. The information can be obtained by experimental measurements and computational simulations. Experimental measurements are reliable but need large labor-effort and time. Therefore, the experimental approach is not feasible as a general design tool. A popular approach of computational simulations is the computational-fluid-dynamics (CFD) method. However, popular models used in the CFD method to calculate turbulence need a fast computer with a large memory.

On the other hand, most building energy analysis programs assume uniform distributions of room air temperature and calculate convective heat exchange coefficient by empirical formulas for simple flows. The energy programs cannot accurately predict energy used by HVAC systems if there is temperature stratification in a space, such as a room with radiant heating/cooling systems, with convective and radiative heating systems, and with displacement ventilation systems. In addition, airflow on room enclosure surfaces is not the same as that in an infinite long heated or cooled surface as often

used to obtain empirical formulas for heat transfer. The heat transfer on room enclosure surface is much more complicated because it can be a combination of forced and natural convection and jet flows. The empirical formulas often fail to calculate accurately heat transfer on the surfaces. Therefore, the temperature distributions of room air and heat transfer on room enclosure surface are important input parameters for a building energy program. A CFD program can calculate the heat transfer.

The CFD methods solve the Navier-Stokes equations for flows. For laminar flows the computed results are accurate and reliable. However, it is difficult to predict turbulent flows. Very fine numerical resolution is required to capture all the details of the indoor turbulent flow. This type of simulation is direct numerical simulation. The direct numerical simulation for a practical flow needs a huge computer system that is not available [1].

Indoor airflow simulations use turbulence models in the CFD approach to compute the mean values. This type of simulation can be done with the capacity and speed of present computers. Eddy-viscosity models are the most popular turbulence models. A typical example of the models is the standard  $k-\epsilon$  model [2]. Most of the models require solving one or more additional differential equations. The computing cost is still large at present. Most HVAC designers and architects

\* Corresponding author. Tel.: +1 617 2537714; fax: +1 617 2536152; e-mail: qchen@mit.edu

$$\begin{aligned}\frac{\partial V_i}{\partial x_i} &= 0 \\ \frac{\partial T}{\partial x_i} &= 0 \\ \frac{\partial C}{\partial x_i} &= 0\end{aligned}\quad (14)$$

• Conventional boundary.

This type of boundary surfaces includes wall, ceiling, and floor surfaces and the surfaces of furniture, appliance, and occupants. If  $x_i$  coordinate is parallel to the surface, the boundary conditions are:

$$\begin{aligned}\tau &= \mu_{\text{eff}} \frac{\partial V_i}{\partial x_j} \\ q &= h(T_w - T) \\ S_C &= C_{\text{source}}\end{aligned}\quad (15)$$

where  $\tau$  = shear stress;  $h$  = convective heat transfer coefficient;  $C_{\text{source}}$  = species concentration source.

The convective heat transfer coefficient is determined from the following equation, which is similar to the Reynolds analogy:

$$h = \frac{\mu_{\text{eff}} C_p}{Pr_{\text{eff}} \Delta x_j}\quad (16)$$

where  $\Delta x_j$  is the distance between the surface and the first grid close to the surface.

#### 4.3. Numerical procedure

A CFD program, PHOENICS [16], is used to solve the conservation equations together with the corresponding boundary conditions. The program discretizes the space into non-uniform computational cells, and the discretized equations are solved with the SIMPLE algorithm [17]. The investigation uses upwind-scheme.

## 5. Application examples

This section demonstrates the new zero-equation model by applying it to predict indoor airflows of:

- Natural convection
- Forced convection
- Mixed convection
- Displacement ventilation

Natural, forced, and mixed convection represent the basic elements of room airflows. For simplicity, two-dimensional cases are selected to demonstrate the zero-equation model. The displacement ventilation case used is three-dimensional with more complicated boundary conditions. The displacement ventilation case is a test of the overall performance of the new model.

### 5.1. Natural convection

For natural convection, the experimental data of Olson and Glicksman [18] as shown in Fig. 1 are used.

Fig. 2 compares the airflow patterns obtained by the zero-equation model, the Lam–Bremhorst [19]  $k-\epsilon$  model, and smoke visualization. The zero-equation model predicts the main stream reasonably well although the boundary layers of the ceiling and floor are thicker. Note that the zero-equation model as well as the  $k-\epsilon$  model predicts the observed reversed flow found beneath the ceiling layer and above the floor layer. The layer thickness are not correct for the zero-equation

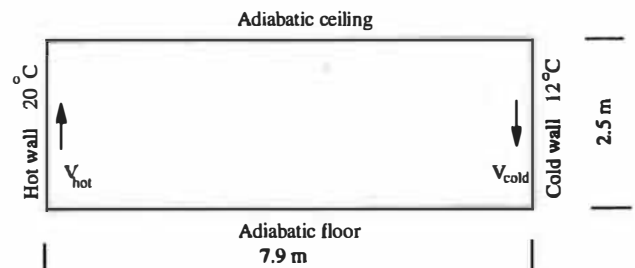


Fig. 1. Sketch and boundary conditions of the natural convection case.

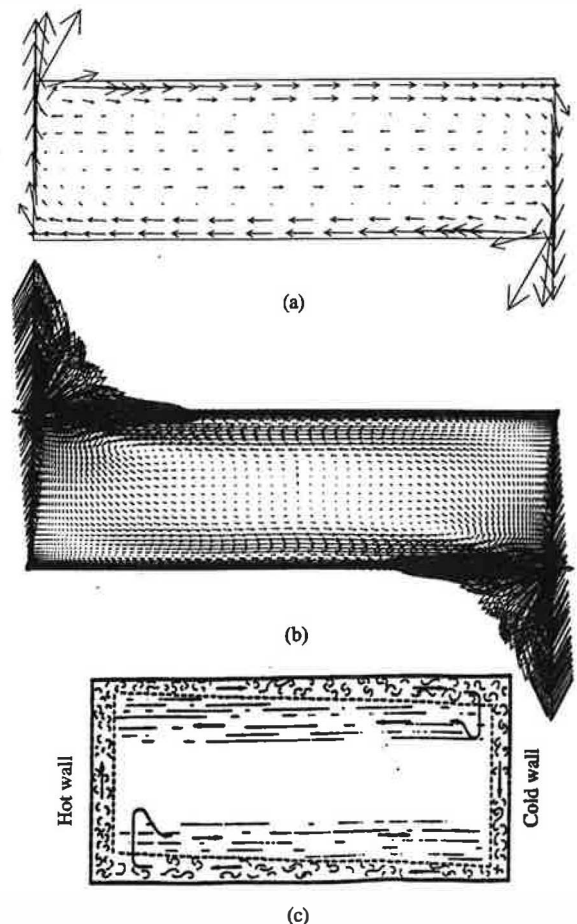


Fig. 2. Comparison of the airflow patterns for natural convection: (a) zero-equation model, (b) the Lam–Bremhorst  $k-\epsilon$  model, (c) smoke visualization.

model due to the large cell size used. However, we found only the Lam–Bremhorst model could predict the reversed flow when we tested quite a few eddy-viscosity models [20].

Fig. 3 presents the dimensionless temperature profiles in the vertical center line. The zero-equation model predicts the temperature profile better than the  $k-\varepsilon$  model in this particular case.

### 5.2. Forced convection

The forced convection case uses the experimental data from Nielsen et al. [21] shown in Fig. 4. The Reynolds number is 5000 based on bulk supply velocity and the height of air supply outlet. The air supply outlet  $h=0.056 H$ , and exhaust inlet  $h'=0.16 H$ .

Fig. 5 compares the airflow patterns by the zero-equation model and the standard  $k-\varepsilon$  model [2]. Since, the standard  $k-\varepsilon$  model has been used extensively in the past and detailed information of the model is widely available, this paper will not repeat all the information. The computed velocity profiles are compared in Fig. 6 with experimental data in two vertical sections  $x/H=1$  and  $x/H=2$  respectively and two horizontal sections,  $y/H=0.972$  (through the air supply outlet) and  $y/H=0.028$  (through the air exhaust inlet). The results of the zero-equation model show a jet decay that is too strong. Hence, the primary flow near the ceiling and the return flow near the floor are smaller than the data. In this case, the  $k-\varepsilon$  model predicts a satisfactory result. Nevertheless, the zero-equation model could predict the secondary recirculation on the upper right corner, though the recirculation is too large. However, the  $k-\varepsilon$  model fails to predict the recirculation.

### 5.3. Mixed convection

The mixed convection case uses the experimental data from Schwenke [22]. The case is similar to the forced convection but the room length is  $4.7 H$  and the height of the air supply outlet  $h=0.025 H$ . The right wall is heated but the ceiling and floor are adiabatic. Schwenke conducted a series measurements with different Archimedes numbers,  $Ar$ , ranging from 0.001 to 0.02.

Fig. 7 compares the computed airflow pattern by the zero-equation model with the standard  $k-\varepsilon$  model. The two results are similar. The airflow pattern is very sensitive to the  $Ar$ . The computed and measured penetration depths,  $x_e$ , vs. different  $Ar$  numbers are compared in Fig. 8. The  $x_e$  is the horizontal distance of air movement along the ceiling before it falls to the floor. The zero-equation model works better in high  $Ar$  but the  $k-\varepsilon$  model better in low  $Ar$ .

### 5.4. Displacement ventilation

Fig. 9 shows the application of the zero-equation model and the standard  $k-\varepsilon$  model for the prediction of room airflow with a displacement ventilation system. The room dimension is 5.6 m long, 3.0 m wide, and 3.2 m high. A convective heat

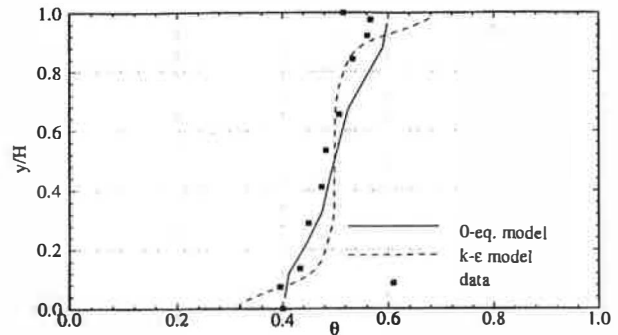


Fig. 3. Comparison of temperature profile in vertical line at the middle of the room with natural convection.

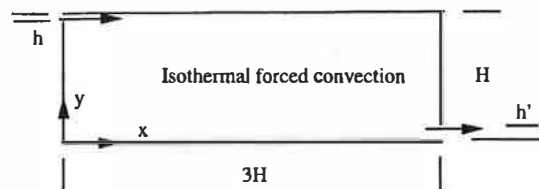


Fig. 4. Sketch of the forced convection case.

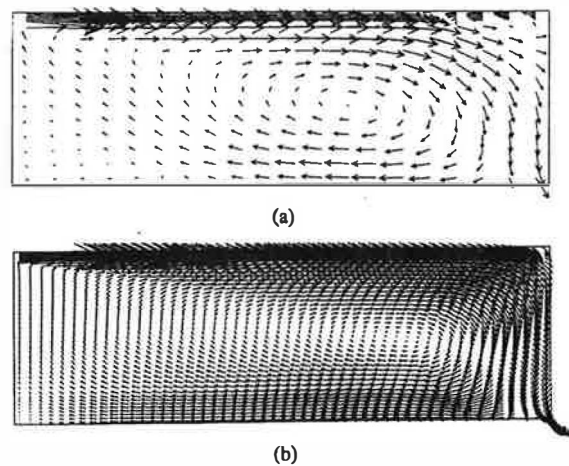


Fig. 5. Comparison of the airflow patterns for the forced convection: (a) zero-equation model, (b) the standard  $k-\varepsilon$  model.

source of 530 W on the window was used to simulate a summer cooling condition. The supply airflow rate was five air-changes per hour. The corresponding supply air temperature was  $19^{\circ}\text{C}$ . A box placed near the table was heated by a 25 W lamp to simulate a person sitting next to the table. The heat strength is considerably lower than that generated from an occupant. However, a helium source was also introduced in the box as a tracer gas to simulate contaminant from the occupant, such as  $\text{CO}_2$  or tobacco smoke. The helium flow rate was 0.5% of the air supply rate. Since helium is much lighter than the air and the helium source was relatively strong in the room, the combined buoyant effect from the thermal source (heat from the lamp) and the mass source (helium) was as strong as that generated from an occupant.

The computations were carried out with different grid numbers with the zero-equation model:  $31 \times 28 \times 26$  (the same as the  $k-\varepsilon$  model),  $16 \times 14 \times 12$ ,  $10 \times 10 \times 10$ , and  $6 \times 7 \times 6$ .

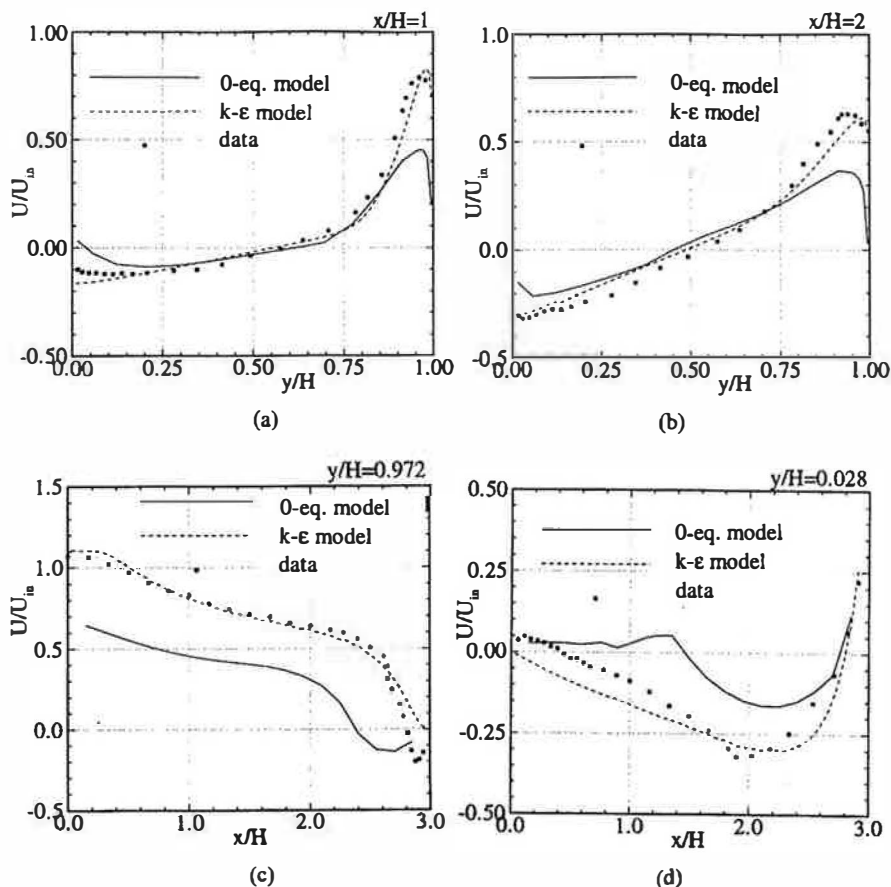


Fig. 6. Comparison of velocity profiles in different sections of the room with forced convection: (a) at  $x/H=1$ , (b) at  $x/H=2$ , (c) at  $y/H=0.972$ , and (d) at  $y/H=0.028$ .

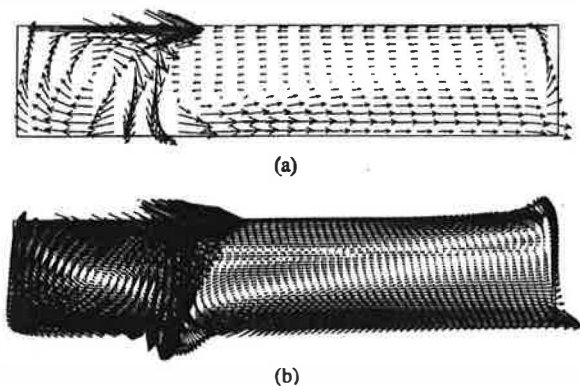


Fig. 7. Comparison of the airflow patterns for the mixed convection: (a) the zero-equation model, (b) the standard  $k-\epsilon$  model.

A grid number of  $16 \times 14 \times 12$  is minimum in order to represent the room geometry, such as the inlet, outlets, window, and table. Fig. 9 shows similar airflow patterns and the distributions of air temperature and helium concentration computed by the zero-equation model with  $16 \times 14 \times 12$  grids and the  $k-\epsilon$  model with  $31 \times 28 \times 26$  grids.

Fig. 10 further compares the computed results with the experimental data. The velocity and temperature profiles are at the center of the room and helium concentration profile at a line near the center of the room. The agreement between

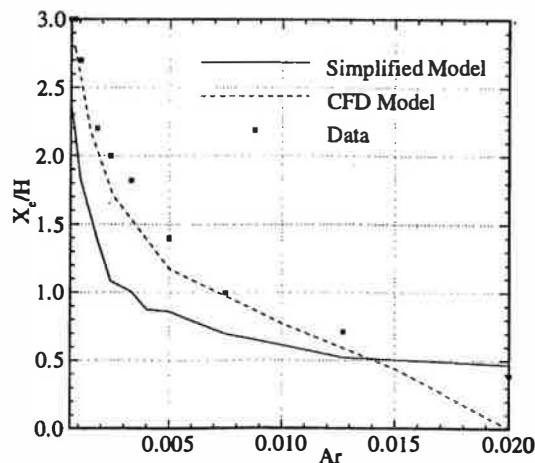


Fig. 8. Comparison of the penetration length vs. Archimedes number for the room with mixed convection.

the computed and measured results is reasonably good. The results are nearly identical between the two models if the grid number is the same. This implies that the new zero-equation model is as good as the  $k-\epsilon$  model for displacement ventilation. However, the model performance depends on flow type. In a separated study to examine the performance of five different  $k-\epsilon$  models, we found that a model may work better in one type of flow but poorer in another type [23]. Therefore,

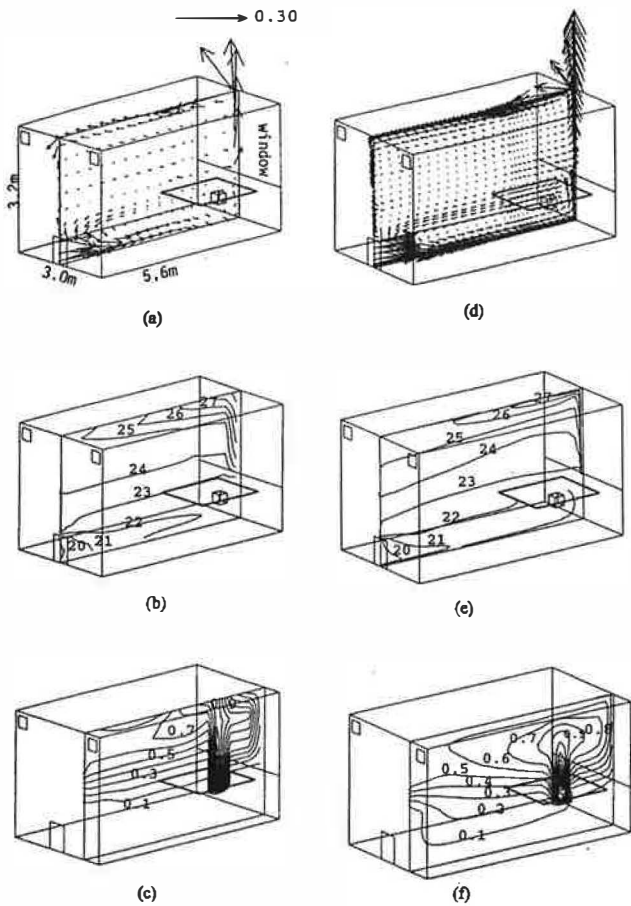


Fig. 9. Comparison of the airflow patterns and distribution of air temperature (°C) and helium concentration (%): (a), (b), and (c) the zero-equation model and (d), (e), and (f) the k-ε model.

we cannot say that the zero-equation model is better than the k-ε model. The main advantage of the zero-equation model is its simplicity and less computing time required, compared with the k-ε model.

It is possible to use a minimum grid number of 6 × 7 × 6 with which the table in the room cannot be represented. The accuracy of the results is relaxed but it does predict the main features of displacement ventilation, such as temperature gradient, non-uniform distribution of contaminant concentration, and higher risk of draft near the inlets at the floor level. The minimal grid number is less than that used in zonal models. Therefore, the zero-equation model has a great potential to be used in an hour-by-hour energy simulation program to take into account the impact of non-uniform temperature distribution on energy consumption.

Note in all of the cases, the zero-equation model, Eq. (7), is exactly the same. No adjustable constants were used in the computations. The zero-equation model is universal for room airflow simulation.

### 6. Discussion

The results show that the k-ε model may predict better results than the new zero-equation model. This is not surpris-

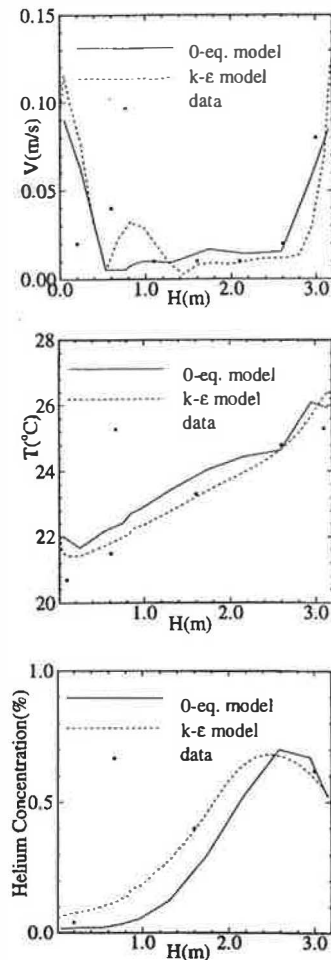


Fig. 10. Comparison of the profiles of air velocity, air temperature, and helium concentration in a vertical line of the room.

Table 1  
Comparison of computing performance of the zero-equation and k-ε models

Case	Model	Grid number	Core memory (bytes)	CPU time (s)
Natural convection	Zero-equation	20 × 10	15,000	18
	k-ε	96 × 60	158,000	3238
Forced convection	Zero-equation	20 × 18	25,000	9
	k-ε	50 × 45	177,000	593
Mixed convection	Zero-equation	25 × 18	31,000	33
	k-ε	70 × 45	263,000	1438
Displacement ventilation	Zero-equation	31 × 28 × 26	555,000	5400
		16 × 14 × 12	75,000	311
		10 × 10 × 10	27,000	119
		6 × 7 × 6	9000	33
	k-ε	31 × 28 × 26	770,000	58,163

ing because the basis of the k-ε model is more solid. The reason to use a zero-equation model is to reduce the computing time used by the k-ε model.

Table 1 shows the total grid number used in the four cases by the zero-equation model and the k-ε models. It also shows the memory needed and CPU time used. The convergence residuals, R, are the same for the zero-equation model and

the  $k-\varepsilon$  models. The present investigation uses  $R < 0.001$  of the mass inflow, for mass continuity and  $R < 0.01$  of energy exchange for temperature.

The computations were conducted on a 486 personal computer. The zero-equation model uses much less memory than the  $k-\varepsilon$  model and is at least 10 times faster than the  $k-\varepsilon$  model. This is because the  $k-\varepsilon$  model solves two more transport equations and the non-linear interaction in all the equations makes it difficult to converge. The results show that most room airflow simulation can be done with a personal computer and the computing time for each case is on the order of a few seconds for a two-dimensional problem and a few minutes for a three-dimensional case.

## 7. Conclusions

This paper proposes a new zero-equation for the prediction of room airflow patterns and the distribution of air temperature and contaminant concentrations. The model is derived from the Navier–Stokes equations. Using the concept of eddy-viscosity, turbulent viscosity is approximated by a length scale and mean velocity. The main difference between the zero-equation model and the  $k-\varepsilon$  model is that the former does not solve transport equations for turbulent quantities. The zero-equation model determines turbulent quantities by an algebraic equation.

The study demonstrates the capability of the zero-equation model by applying it to predict the airflow with natural convection, forced convection, mixed convection, and displacement ventilation in rooms. The predicted results are compared with experimental data and the results with the standard  $k-\varepsilon$  model. The zero-equation model can predict indoor airflow patterns and the distributions of air temperature and contaminant concentrations with reasonable accuracy.

Since the zero-equation model does not solve transport equations for turbulence, the computer memory needed is much smaller, and the convergence speed is 10 times faster than that of the  $k-\varepsilon$  model. With the zero-equation model, simulation of a three-dimensional, steady-state flow in a room can be made in a personal computer.

## Acknowledgements

The investigation is supported by the US National Science Foundation Grant No. CMS-9623864.

## References

- [1] F.T.M. Nieuwstadt, J.G.M. Egges, R.J.A. Hanssen, M.B.J.M. Pourquie, Direct and large-eddy simulations of turbulence in fluids, *Future Generation Comput. Syst.* 10 (1994) 189–205.
- [2] B.E. Launder, D.B. Spalding, The numerical computation of turbulent flows, *Comp. Meth. Appl. Mech. Energy* 3 (1974) 269–289.
- [3] L. Prandtl, Über die ausgebildete Turbulenz, *ZAMM* 5 (1925) 136–139.
- [4] E.R. van Driest, On turbulent flow near a wall, *J. Aeronaut. Sci.* 23 (1956) 1007.
- [5] F.H. Clauser, The turbulent boundary layer, *Advances in Applied Mechanics: IV*, Academic Press, New York, 1956, pp. 1–51.
- [6] M.P. Escudier, The distribution of mixing-length in turbulent flows near walls, Heat Transfer Section Report TWF/TN/12, Imperial College, 1966.
- [7] S. Corrsin, A.L. Kistler, The free-stream boundaries of turbulent flows, *NACA TN 3133* (1954).
- [8] P.S. Klebanoff, Characteristics of turbulence in a boundary layer with zero pressure gradient, *NACA TN 3178* (1956).
- [9] T. Cebeci, A.M.O. Smith, *Analysis of turbulent boundary Layers*, Series in Applied Mathematics and Methods: XV, Academic Press, 1974.
- [10] D.C. Wilcox, *Turbulence modeling for CFD*, DCW Industries, 1993, p. 51.
- [11] B.S. Baldwin, H. Lomax, Thin-layer approximation and algebraic models for separated turbulent flows, *AIAA Paper*, Huntsville, AL, 1978, pp. 78–257.
- [12] A.A. Ameri, A. Arnone, Prediction of turbine blade pass heat transfer using a zero and a two-equation turbulence model, *ASME Proceedings of the International Gas Turbine and Aeroengine Congress and Exposition*, Paper 94-GT-122, June 13–16, Hugas, Neth ASME, New York, 1994, pp. 1–8.
- [13] D.E. Nikitopoulos, E.E. Michaelides, Phenomenological model for dispersed bubbly flow in pipes, *AIChE J.* 41 (1) (1995) 12–22.
- [14] H. Liu, M. Ikehata, Computation of free surface waves around an arbitrary body by a Navier–Stokes solver using pseudocompressibility technique, *Int. J. Numerical Methods Fluids* 19 (5) (1994) 395–413.
- [15] S.-W. Chyou, C.A. Sheicher, Can one- and two-equation models be modified to calculate turbulent heat transfer with variable properties?, *Ind. Eng. Chem. Res.* 31 (3) (1992) 756–759.
- [16] *PHOENICS Reference Manual*, CHAM, London, 1996.
- [17] S.V. Patankar, *Numerical Heat Transfer and Fluid Flow*, Hemisphere Publishing, New York, 1980.
- [18] D.A. Olson, L.R. Glicksman, Transient natural convection in enclosures at high Rayleigh number, *ASME J. Heat Transfer* 113 (1991) 635–642.
- [19] C.K.G. Lam, K. Bremhorst, A modified form of the  $k-\varepsilon$  model for predicting wall turbulence, *ASME J. Fluid Eng.* 103 (1981) 456–460.
- [20] W. Xu, Q. Chen, Numerical simulation of air flow in a room with differentially heated vertical walls, *ASHRAE Trans.* 104 (1) (1998).
- [21] P.V. Nielsen, A. Restivo, J.H. Whitelaw, The velocity characteristics of ventilated rooms, *J. Fluid Eng.* 100 (1978) 291–298.
- [22] H. Schwenke, Ueber das Verhalten elener horizontaler Zuluftstrahlen im begrenzten Raum, *Luft- und Kältetechnik* 5 (1975) 241–246.
- [23] Q. Chen, Comparison of different  $k-\varepsilon$  models for indoor airflow computations, *Numerical Heat Transfer, Part B: Fundam.* 28 (1995) 353–369.